

Lazy Probabilistic Roadmaps Revisited

Miquel Ramirez ✉ 

School of Electric and Electronic Engineering, University of Melbourne, Australia

Daniel Selvaratnam ✉ 

Division of Decision and Control Systems, School of Electrical Engineering and Computer Science, KTH Royal Institute of Technology, Stockholm

Chris Manzie ✉

School of Electric and Electronic Engineering, University of Melbourne, Australia

Abstract

This paper describes a revision of the classic Lazy Probabilistic Roadmaps algorithm (Lazy PRM), that results from pairing PRM and a novel Branch-and-Cut (BC) algorithm. Cuts are dynamically generated constraints that are imposed on minimum cost paths over the geometric graphs selected by PRM. Cuts eliminate paths that cannot be mapped into smooth plans that satisfy suitably defined kinematic constraints. We generate candidate smooth plans by fitting splines to vertices in minimum-cost path. Plans are validated with a recently proposed algorithm that maps them into finite traces, without need to choose a fixed discretization step. Trace elements exactly describe when plans cross constraint boundaries modulo arithmetic precision. We evaluate several planners using our methods over the recently proposed BARN benchmark, and we report evidence of the scalability of our approach.

2012 ACM Subject Classification Computing methodologies → Planning and scheduling

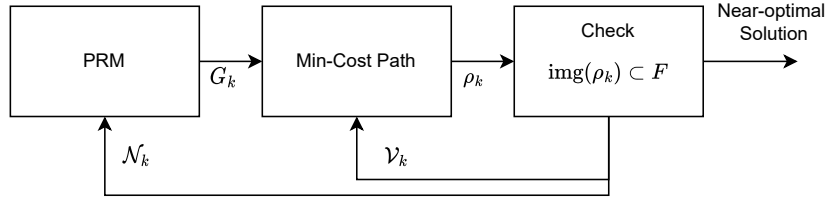
Keywords and phrases Motion Planning, Combinatorial Optimization, Formal Methods

1 Introduction

The problem of planning the motions of a moving object like a robot is, in its most basic form, that of finding trajectories that satisfy *constraints*. The classic example of constraint in robot motion planning is that of *obstacles*, objects like walls, etc., that we want our controlled robot to avoid being in contact with or too close by. Besides ensuring that trajectories and constraints are disjoint, we also want the former to minimize some given index of performance, that ranks trajectories according to their desirability.

In this paper we look at motion planning as an infinite optimization problem [1], that is laid upon a given set $C \subset \mathbb{R}^d$, the robot configuration space. Informally, solutions (*plans*) must stay within the subset $F := C \setminus O$, where O represents the obstacles. Plans are piece-wise defined curves $\rho : [0, 1] \rightarrow C$, that connect a given initial configuration $q_0 \in F$ and target set $F_* \subset F$. Plans must also belong to a set Π given by suitably defined *kinematic and dynamic* constraints [2]. The task at hand is to (1) select plans that minimize a smooth *objective function*, and (2) verify whether the image of ρ is contained in F , i.e. $\text{img}(\rho) \subset F$. In this paper we require plans to be C^2 -continuous, so their first and second derivatives exist. This enables the assumption that a suitably designed local controller (see [3] for an expressive and recent framework) that can steer the robot within a small neighborhood of ρ without overlapping with any obstacles. This assumption holds, for example, when the robot dynamics are given by a differentially flat non-linear dynamical system [4].

The complexity of motion planning motivates its decomposition into more tractable subproblems, all the while striking compromises on the optimality of solutions and completeness of the resulting algorithm. A concrete and classic example of such a decomposition is Bohlin and Kavraki's Lazy Probabilistic Roadmaps (Lazy PRM) [5]. Figure 1 depicts Bohlin and Kavraki's iterative algorithm, and the order in which subproblems are solved. For the k th iteration, the first subproblem selects a *geometric graph* [6] $G_k = (V_k, E_k)$. Vertices $V_k \in C$ (points) and edges E_k (point-to-point curves) in G_k identify a finite subset of decision variables of the infinite motion planning problem. The graph



■ **Figure 1** Bohlin and Kavraki’s decomposition of motion planning. \mathcal{N}_k and \mathcal{V}_k are, respectively, search directions and no-good constraints generated when the incumbent plan ρ_k is found to overlap obstacles.

G_k is then used to formulate a *minimum-cost path problem* [7], where optimal solutions correspond to paths (piecewise functions) ρ_k in G_k that minimize a suitably defined cost function and connect q_0 with F_* . If such a ρ_k exists, it is necessary to check whether $\text{img}(\rho_k) \subset F$. This check fails whenever ρ_k overlaps with some constraint O_i . In this case the algorithm backtracks, and two new constraints are generated [8, 9] for the roadmap and minimum-cost path search. For the former, a neighbourhood $\mathcal{N}_k \subset \mathcal{C}$ is defined, that *directs* PRM towards geometric graphs with vertex set $V \supset V_k$ that may support edges and paths around constraint O_i . For the minimum-cost path problem, a *no-good* constraint $\mathcal{V}_k \subset E_k$ is generated that removes all solutions that would violate constraint O_i . A supergraph G_{k+1} of G_k is then selected, and the procedure repeats until a feasible path is found. This algorithm can be shown to be both probabilistically complete (PC) and asymptotically optimal (AO) in a trivial manner from the results by Karaman and Frazzoli [10] and later follow-ups [11].

1.1 Contributions

This paper expands Bohlin and Kavraki’s Lazy PRM algorithm by (1) doing away with the need to sample ρ at a fixed rate to verify whether $\text{img}(\rho) \subset F$ (section 6.1), (2) solving a minimum-cost path problem augmented with dynamically generated constraints via branch-and-cut (section 4), and (3) enforcing kinematic constraints by means of fitting a C^2 curve to waypoints (section 5) and checking if constraints on $\dot{\rho}$ are violated (section 6.3).

The problem of establishing whether $\text{img}(\rho) \cap O \neq \emptyset$ can only be solved [12] when ρ and O are described by a system of polynomial equations. Testing emptiness is then reduced to root-finding. However, there is no analytical solution to polynomial root-finding when the degree is greater than 5 [13, Abel-Ruffini Theorem]. We follow an alternative strategy [14]: instead of locating roots, we seek a sequence of *root isolating intervals* [15] enclosing them.

Additionally, we generalize Lazy PRM by noting that it is an application of the *branch-and-cut* (BC) method for combinatorial optimization [9, 16, 17]. BC algorithms consist of two components: *branch-and-bound* (BB) search and a suitably defined *cutting plane* procedure. The latter produces *cuts*, linear constraints, that prune away solutions that violate problem constraints that cannot be represented explicitly. In the context of Lazy PRM, cuts rule out sequences of edges in the geometric graph that violate kinematic constraints, or are shown to not satisfy kinematic and geometric constraints simultaneously.

1.2 Structure of the Paper

The paper is structured as follows. We start by introducing a number of definitions we rely upon. We then introduce our extension to Bohlin and Kavraki’s Lazy PRM, detailing the ways in which we depart from Figure 1, the algorithms or optimization problems used. We then report the results of a comprehensive empirical evaluation over a recently proposed benchmark for motion planning

algorithms [18]. We end the paper covering key related and future work.

2 Mathematical Framework

We provide now several basic definitions that will be used throughout the paper. Let \mathbb{Q} be the set of rational numbers, and \mathbb{R} the reals. Given two *points* $x, y \in \mathbb{R}^d$, we denote by $\|x - y\|_2$ the l_2 -norm, or *Euclidean distance* between them. Let

$$X \oplus Y := \{x + y \mid x \in X, y \in Y\}$$

be the *Minkowski sum* of $X \subseteq \mathbb{R}^d$ and $Y \subseteq \mathbb{R}^d$. $\mathcal{B}_r(x) := \{y \in \mathbb{R}^d \mid \|y - x\|_2 \leq r\}$ denotes the d -dimensional *closed ball* of radius $r \geq 0$ centered at $x \in \mathbb{R}^d$. Similarly, given a function $\pi : [0, 1] \rightarrow \mathbb{R}^d$, we define $\mathcal{B}_r(\pi) = \bigcup_{t \in [0, 1]} \mathcal{B}_r(\pi(t))$. Given a subset $C \subset \mathbb{R}^d$ we denote by $\text{vol}(C)$ its Lebesgue measure or *volume*. Given a set of points $X \subset C$, then $D(X, C)$ is the l_2 -*dispersion* of X

$$\begin{aligned} D(X, C) &:= \sup_{q \in C} \min_{q' \in X} \|q - q'\|_2 \\ &= \sup\{r > 0 : \exists q \in C \text{ s.t. } \mathcal{B}_2(q, r) \cap X = \emptyset\}; \end{aligned} \quad (1)$$

in words, the radius r of the largest ball $\mathcal{B}_r(y)$ we can embed within $C \setminus X$ around $y \notin X$.

Let $R[x_1, \dots, x_d]$ denote the ring of polynomials in the variables x_1, \dots, x_d with coefficients in R , where R can be any commutative ring with multiplicative identity [13, Chapter 9]. Thus, $\mathbb{R}[t]$ is the ring of *univariate polynomials* with real-coefficients, and $\mathbb{Q}[x_1, \dots, x_d]$ the ring of *multivariate polynomials* in d variables with rational coefficients.

A *graph* $G = (V, E)$ is given by its vertex V and edge $E \subseteq V \times V$ sets, with $v \neq w$ for every edge $(v, w) \in E$. If $(v, w) \in E$, we say that v and w are *adjacent*, and that (v, w) is an *outgoing* (resp. *incoming*) edge for v (resp. w). A *path* in G is a sequence $p = v_0, v_1, \dots, v_n$ of *distinct elements* of V such that $(v_i, v_{i+1}) \in E$ for all $0 \leq i < n$. The set of all such sequences is $\text{Paths}(G)$. The graph G is *connected* if for any two distinct vertices $u, v \in V$ there is a path $p = w_0, \dots, w_n$ such that $u = w_0$ and $v = w_n$.

2.1 Motion Planning

We now fully formalize and describe the discussion of motion planning problems in the Introduction. Let the open set $C \subset \mathbb{R}^d$ be the *robot configuration space*, that is, the set of d -dimensional real vectors representing robot states (pose, battery level, etc.), and let $O \subset C$ be a closed subset of C that correspond to sets of potential robot states (overlap with obstacles, minimum battery levels, etc.) to be avoided. O consists of m connected components O_i s.t. $O = \bigcup_{i=1}^m O_i$, and each O_i is a *semi-algebraic set* of the form

$$O_i := \bigcap_{j=1}^{m_i} \{x \in C : g_j^i(x) \leq 0\}. \quad (2)$$

In words, each obstacle O_i is given by the intersection of m_i sets, each defined in terms of *constraints* $g_j^i(x) \leq 0$, where each $g_j^i : \mathbb{R}^d \rightarrow \mathbb{R}$ is a multivariate polynomial. The set of admissible or valid robot states, or *freespace*, is then the open set $F = C \setminus O$.

Motion planning is the problem of finding a continuous function $\rho : [0, 1] \rightarrow C$, or *plan*, that connects a given initial state $q_0 \in F$, to a *goal region* $F_\star \subset F$ s.t. $\text{vol}(F_\star) > 0$. That is, a plan belonging to a suitably defined *plan domain*, $\rho \in \Pi$, that verifies $\rho(0) = q_0$, $\rho(1) \in F_\star$, and every

4 Lazy Probabilistic Roadmaps Revisited

point $\rho(t)$ lies within F . Additionally, we will require ρ to minimize a given *objective* function $f : \Pi \rightarrow \mathbb{R}$, which ranks the plans in Π . We use the following notation to describe precisely the set of plans ρ that solve optimally this problem

$$\min_{\rho \in \Pi} f(\rho) \quad (3a)$$

$$\rho(0) = q_0, \rho(1) \in F_* \quad (3b)$$

$$\mathcal{B}_{\delta_i}(\rho) \subset C \setminus O_i, \quad i = 1, \dots, m \quad (3c)$$

where $\delta_i \geq 0$, or *clearance*, indicates the minimum distance from a point $\rho(t)$ to the boundary of a set O_i (2)¹ *Plan domains* Π are defined in terms of m' *differential constraints* [19, Chapter 13]

$$\Pi := \{\rho : g_i(\rho(t), \dot{\rho}(t), \ddot{\rho}(t)) \leq 0, i = 1, \dots, m'\} \quad (4)$$

where ρ is a C^2 -continuous function and each $g_j^i : \mathbb{R}^{3d} \rightarrow \mathbb{R}$. Candidate plans ρ are defined as *piecewise functions* in Π that follow from the concatenation of a finite sequence of *actions* $(a_i)_{i=1}^N$, $1 \leq i \leq N$, where $a_i : [0, 1] \rightarrow C$. We observe that for any ρ with more than one action, C^2 -continuity is not trivial, and we discuss in section 5 how to obtain efficiently piecewise functions with the desired properties. Finally, we locate points on $\rho(t)$ using

$$\rho(t) = a_{\lceil nt \rceil}(nt - \lfloor nt \rfloor) \quad (5)$$

► **Example 1.** A well-studied special case of Problem (3) is known as *geometric motion planning*, where Π is the set of continuous, *piecewise-defined linear functions*. Thus, each $a_i(t)$ is a vector of *linear* polynomials of the form

$$a_i(t) = (q_{i+1} - q_i)t + q_i,$$

where $q_1, \dots, q_N \in \mathbb{R}^d$ are *waypoints*. The plans $\pi \in \Pi$ are required to have C^0 -continuity; i.e., $a_i(0) = a_{i+1}(1)$, for $i = 1, \dots, N - 1$.

2.2 Probabilistic Roadmaps and Random Geometric Graphs

- 1: **procedure** PRM($G_k = (V_k, E_k), \mathcal{X}$)
- 2: choose q_k from $X_k \in \mathcal{X}, E \leftarrow \emptyset$
- 3: **for** $q \in (\mathcal{B}_{r_k}(q_k) \cap V_k)$ **do**
- 4: choose $\lambda \in \Lambda$ s.t. $\lambda(0) = q_k$ and $\lambda(1) = q$
- 5: $E \leftarrow E \cup \{(q_k, q)\}$
- 6: **end for**
- 7: return $G_{k+1} = (V_k \cup \{q_k\}, E_k \cup E)$
- 8: **end procedure**

■ **Figure 2** Graph search or “learning” component of the Probabilistic Roadmaps (PRM) algorithm [20] as an iterative geometric graph optimization algorithm.

The key algorithmic development leading to general, scalable algorithms for motion planning was the invention of the Probabilistic Roadmaps (PRM) algorithm [21, 22]. As noted in the Introduction, motion planning problems (3) cannot be solved directly, as it is necessary to identify a *finite subset*

¹ We note that clearance does not need to be a global parameter.

of the decision variables and constraints. PRM decomposes (3) into two subproblems: a *learning* subproblem, where a *random geometric graph* G [6] meeting some requirements is sought, and a *combinatorial optimization* problem whose solutions are paths $p \in Paths(G)$ such that a certain objective function, typically the sum of lengths of the edges, is minimized [7]. Before discussing the PRM algorithm, which is given in Figure 2, we formalize the learning subproblem as that of searching over an infinite set of geometric graphs \mathcal{G} , looking for those that meet the following criteria

$$\min_{G=(V,E) \in \mathcal{G}(S)} D(V, S) \quad (6a)$$

$$\text{such that } V \subset S, E \subset \Lambda \quad (6b)$$

$$q_0 \in V, F_\star \cap V \neq \emptyset \quad (6c)$$

Solutions or *roadmaps*, are random geometric graphs $G = (V, E)$ required, via constraint (6b), to be such that the vertex set is a subset of topological space S , and edges in E correspond to functions $\lambda \in \Lambda$, $\lambda : [0, 1] \rightarrow S$, or *local plans*. Solutions (graphs) G are also required, via constraint (6c), to cover the initial state q_0 and the set of goal states F_\star . As noted by Janson et al. [23], ℓ_2 -dispersion (1) for vertex set V describes how well the former covers the set S , and therefore bounding how close any plan associated with a path $p \in Paths(G)$ can approximate the (unattainable) optimal cost for Problem (3). Many formulations of (6) exist in the literature, with significantly different properties.

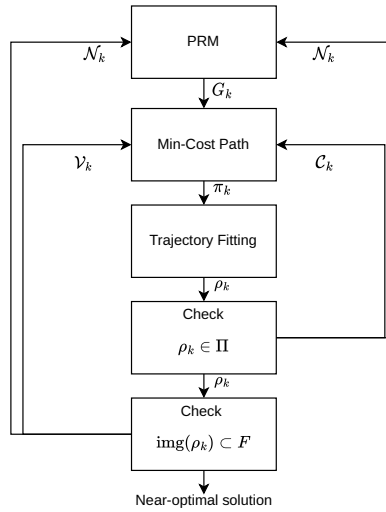
► **Remark 2.** In the original PRM paper [20], $S = F$ and $\Lambda = \{\rho \in \Pi : \text{img}(\rho) \subset F\}$, so that paths $p \in Paths(G)$ map directly onto solutions for Problem (3). In contrast, Bohlin and Kavraki set $S = C$ and Λ to be the set of local plans $\lambda : [0, 1] \rightarrow C$, so that paths $p \in Paths(G)$ may or not map onto solutions for Problem (3).

We adapt the classic descriptions of PRM (Figure 2) in the literature to be an iterative algorithm, that generates a sequence of geometric graphs G_k , $k = 0, 1, \dots$. The initial graph G_0 is given by the tuple $(\{q_0, q_\star\}, \emptyset)$, where q_\star is a suitably chosen state in F_\star . Each iteration Algorithm 2 chooses G_{k+1} , a supergraph of G_k , by adding a new vertex $q_k \in S$ and as many edges $\lambda \in \Lambda$ as possible that connect q_k with points $q' \in V_k$ in a suitably defined neighborhood centered at q_k . Line 2 in Figure 2 initializes the iteration by *sampling* state q_k from a *sequence* $\mathcal{X} := X_0 X_1 \dots X_k \dots$ of *random variables* whose distribution support² is S . Line 3 enumerates the elements in the neighborhood of q_k , which is defined by the set of existing vertices V_k and a ball of radius $r_k > 0$. This parameter, or *connection radius*, decreases monotonically as k increases, ensuring that as G becomes bigger, ℓ_2 -dispersion [22, 23] is reduced. Importantly, the schedule for r_k cannot be arbitrary as it greatly affects the *convergence* of G_k to a graph where q_0 and some vertices $F_\star \cap V$ belong to the same connected component [22]. Edges (local plans λ) are added in lines 4 and 5 of Figure 2. Depending on the definition of Λ (see above), no valid local plan may exist, and then no edge is added.

3 Revisiting Lazy PRM

We revisit the notion of Bohlin and Kavraki's Lazy PRM, proposing a different structuring into subproblems, as well as novel methodologies to address them. These changes and additions are depicted in Figure 3. First, we set $S = F$ and choose Λ in Problem (6) as the set of linear piecewise functions discussed in Example 1. From the resulting geometric graph G_k , we formulate a Constrained Min-Cost Path (CMCP) problem (section 4), and seek its optimal solutions, paths $\pi_k \in Paths(G_k)$,

² We note that the support of a random variable X taking values in \mathbb{R}^n is the set $\{x \in \mathbb{R}^n : P_X(\mathcal{B}_r(x)) > 0, \text{ for all } r > 0\}$, and more generally, the smallest closed set such that $P_X(C) = 1$, where $P_X(S)$ is the probability of X taking as a value an element of set S .



■ **Figure 3** Revised Lazy PRM, see text for details and discussion.

which we will refer to as *geometric plans*. These do not in general correspond with plans $\rho \in \Pi$, so we need to determine if π_k can be mapped onto some element of Π . The existence of this mapping, specified on elements, is verified in two steps. First, we choose a smooth function ρ_k , which we will be referring to as *smooth plan*, by solving a (convex optimization) *trajectory fitting* problem [24] (section 5). This choice is constrained so that ρ_k is C^2 -continuous and traces through each vertex in π_k . Second, we then check if suitably defined kinematic constraints on ρ_k are satisfied, certifying that there is a match between π_k and at least one element in Π (section 6.3). If this check fails, and ρ_k is proven to not be an element of Π , a cut \mathcal{C}_k is generated and added to the set of constraints of the CMCP problem. Proving that $\rho_k \in \Pi$ is not sufficient, as we need to check if $\text{img}(\rho_k) \subset F$ (section 6.1), ensuring that both kinematic and geometric constraints are satisfied simultaneously. If this second test fails, a new cut \mathcal{V}_k is obtained and added to the constraints of the CMCP. Both of these tests implement the cutting plane component of our BC algorithm. Finally, whenever the check $\rho_k \in \Pi$ (resp. $\text{img}(\rho) \subset F$) is passed by the candidate smooth plan ρ_k , cuts $\mathcal{C}_k = \emptyset$ (resp. $\mathcal{V}_k = \emptyset$).

► **Remark 3.** In this paper it is assumed that checking local plans (straight lines) $\lambda \subset F$ to obtain the geometric graphs G_k in Figure 3 is computationally efficient. When this assumption does not hold, one can revert to the formulation of Problem (6) used by Bohlin and Kavraki. The algorithm in Figure 3 does not need to change, as the procedure described in section 6.1 is guaranteed to reject plans ρ_k s.t. $\text{img}(\rho) \cap O \neq \emptyset$.

The algorithm in Figure 3 iterates for a set amount of time, possibly finding several valid plans ρ_k with monotonically decreasing costs. The selection of geometric graphs G_k is steered by a sampling sequence \mathcal{X} of random variables X_k . Each of these chooses, with equal probability, either points $q \in F$ according to distribution $P_{X_k}(F) = 1$, or points $q \in \mathcal{N}_k \subset F$ from *search direction* \mathcal{N}_k . These are defined in terms of the vertices featuring in cuts \mathcal{V}_k and \mathcal{C}_k generated so far (section 6.4). This heuristic, analogous to the notion of *activity-based* branching heuristics [25] in discrete optimization, ensures that geometric graphs G_k with paths that are structurally similar to those rejected by previous cuts are frequently considered without compromising completeness.

4 Constrained Min-Cost Path Problems

We start by introducing the formulation of minimum-cost path (MCP) as an Integer Linear Program (ILP) [16] where costs are defined over the edges in a path. Given a geometric graph $G = (V, E)$, the task is to find the path $p = q_0 q_1 \dots q_i \dots q_N q_t$ in the graph $G' = (V', E')$ that follows from adding a dummy vertex q_t and additional edges $\{(q_i, q_t) : q_i \in V \cap F_\star\}$, and that minimizes $f(p)$, a linear function. The set of all possible paths is represented by a vector of *decision variables* $x \in \{0, 1\}^{|V|^2}$, so each x_{ij} allows to choose whether edge (q_i, q_j) is in the solution path p . The objective $f(p)$ is defined as the inner product of x with a vector $c \in \mathbb{R}^{|V|^2}$ of *edge costs*. These costs can be, for instance, the *arc-length* of the local plan λ_{ij} connecting q_i and q_j . The choice of which edges to use is restricted by a number of constraints that follow from the structure of the graph G , so the *optimal cost* $\phi(G)$ of the MCP for graph G instance is described by the following mathematical program

$$\phi(G) := \min_x \sum_{i=1}^{|V|} \sum_{j=1}^{|V|} c_{ij} x_{ij} \quad (7a)$$

$$\text{such that } \sum_{(q_0, q_j) \in E} x_{0j} = 1 \quad (7b)$$

$$\sum_{(q_i, q_k) \in E} x_{ik} - \sum_{(q_k, q_j) \in E} x_{kj} = 0 \quad (7c)$$

$$\sum_{q_i \in V_\star} x_{it} = 1 \quad (7d)$$

$$x_{ij} = 0, \text{ for } i, j, \text{ s.t. } (q_i, q_j) \notin E \quad (7e)$$

► **Remark 4.** The above is a trivial variation on the classic formulation of shortest-path problems in graphs as a special case of minimum-cost flow problems [26].

The objective function (7a) is a linear function as introduced above, where each coefficient c_{ij} corresponds to the value of a cost function $f : \Lambda \rightarrow \mathbb{R}$. Constraint (7b) follows from the trivial fact that all valid paths must start at vertex q_0 , therefore exactly one of q_0 outgoing edges must be in the path. *Flow constraints* (7c) range over every $q_k \in V$ but q_0 , and ensure that if an incoming edge of q_k is in the selected path p , then one of its outgoing edges must also be in p . Constraint (7d) ensures that the path p ends at the dummy vertex q_t , and constraint (7e) prevents selecting into p possible edges for which no local plan has been found.

► **Remark 5.** ILPs like Problem (7) can be efficiently solved via generic algorithms for Integer Linear and Dynamic Programming based on Branch-and-Bound [26, 27]. The choice of algorithm being determined by (1) the nature of the coefficients of the cost function, (2) availability of good cost relaxations to orient the search for solutions, (3) the maximal number b of outgoing edges from any vertex in V , or *branching factor*, and (4) the least number d of actions (edges) in optimal plans, or *depth* of optimal solutions.

4.1 Branch-and-Cut over Probabilistic Roadmaps

As noted in section 3, the definition of S and Λ in Problem (6), determines whether there exists an injective mapping between solutions π to constraints (7b)–(7e) and plans ρ that solve Problem (3). Recovering this property would require us to augment Problem (7) with constraints

$$\sum_{(q_i, q_j) \in \mathcal{E}} x_{ij} \leq |\mathcal{E}| - 1 \quad (8)$$

for each possible subset $\mathcal{E} \subset E_k$ of the edges in graph G_k that (1) appear contiguously in some solution of Problem (7) and (2) there is no $\rho \in \Pi$ tracing the vertices in \mathcal{E} . Doing so is only feasible for very small graphs, as the number of sets \mathcal{E} to consider is exponential on the number of vertices of G_k . Besides the sheer number of edge sets to test and constraints to be added, only a very small fraction of these will be relevant to optimal solutions of Problem (7), so the computational effort invested in verifying every path and sub-path is not amortised. Avoiding such wasted effort is one of the key motivations for us to look again into Lazy PRM.

Branch-and-cut (BC) was originally proposed in the context of Mixed-Integer Linear Programming [17] as a way to manage combinatorial explosions in the number of sub-tour elimination constraints [28] required to formulate the Travelling Salesman Problem (TSP). We observe that BC is directly applicable to motion planning over probabilistic roadmaps, generalizing the results of Bohlin and Kavraki, as the problem of selecting best paths in G_k can be trivially described by an integer linear problem. Concrete BC algorithms for motion planning thus need to (1) decide what constraints need to be *separated* from the ones used to identify optimal solutions, and (2) specify one or more procedures to check when an optimal solution for Problem (7) violates any of the separated constraints, generating *cuts* (8) that are added to (7b)–(7c). We discuss these procedures and the cuts generated in section 6.

5 Trajectory Fitting

The next subproblem we address is that of *trajectory fitting*, in which we map geometric, C^0 -continuous plans π_k , a sequence of local plans λ selected by optimal solution of CMCP problems, into smooth, C^2 -continuous plans ρ_k . We approach this problem as a *function fitting* problem [24], where we select a member of a finite dimensional subspace of functions, a *superset* of plan domain Π in Problem (3), that is the *best fit* given some data (waypoints q_i , $i = 0, \dots, N$ in π_k) and requirements (continuity of the derivatives at each waypoint). Formally, given a family of *basis functions* $\eta_1, \dots, \eta_n : \mathbb{R} \rightarrow \mathbb{R}$, we seek a function

$$\eta(t) = \theta_1 \eta_1(t) + \theta_2 \eta_2(t) + \dots + \theta_n \eta_n(t), \quad (9)$$

where the coefficients $\theta_1, \dots, \theta_n \in \mathbb{R}^d$ parameterize the subspace of functions and become the decision variable for an optimization problem. In line with the mathematical tractability and robot controllability concerns expressed in the Introduction, we consider polynomial basis functions

$$\eta_l(t) = t^{l-1}, \quad l = 1, \dots, n \quad (10)$$

matching the requirements stated in section 2.1. We now observe that the geometric plan π_k is defining a *triangulation* of the domain of plans (functions) ρ , the interval $[0, 1]$. That is, geometric plan $\pi = q_0 q_1 \dots q_i \dots q_N$ is partitioning $[0, 1]$ into N disjoint *simplices* (lines) comprised between the grid points $g_0 = 0, g_1 = 1/N, \dots, g_i = i/N, \dots, g_N = 1$. A piece-wise polynomial then can be obtained directly by fitting to each of the simplices a function like (9) that is defined over the basis (10), requiring the desired continuity constraints at the boundaries between each simplex. In this paper we consider, the polynomial basis with $l = 4$, that is, smooth plans ρ are *cubic splines*. The constraints and analysis that follows can be trivially extended into higher degree basis (like $n = 6$), or other types of C^2 -continuous spline curves, like B-splines [29].

Let $\theta = (\alpha, \beta, \kappa, \delta) \in \mathbb{R}^4$, then for each dimension $j = 1, \dots, d$ the polynomial piece a_i , $i = 0, \dots, N - 1$, is defined in terms of parameters θ_{ij} as follows:

$$a_{ij}(t) := \alpha_{ij} t^3 + \beta_{ij} t^2 + \kappa_{ij} t + \delta_{ij}, \quad j = 1, \dots, d \quad (11)$$

For each simplex $i = 0, \dots, N - 1$ and $j = 1, \dots, d$ we require that the endpoints match adjacent waypoints, e.g. $\rho_{ij}(0) = q_{ij}$ and $\rho_{ij}(1) = q_{i+1j}$, which translates into the following linear constraints

$$\delta_{ij} - q_{ij} = 0 \quad (12)$$

$$\alpha_{ij} + \beta_{ij} + \kappa_{ij} + \delta_{ij} - q_{i+1j} = 0 \quad (13)$$

C^2 -continuity is enforced by requiring that $\dot{\rho}_{ij}(1) = \dot{\rho}_{i+1j}(0)$, and $\ddot{\rho}_{ij}(1) = \ddot{\rho}_{i+1j}(0)$ for $i = 0, \dots, N - 2$ and $j = 1, \dots, d$, that translates into constraints

$$3\alpha_{ij} + 2\beta_{ij} + \kappa_{ij} - \kappa_{i+1j} = 0 \quad (14)$$

$$6\alpha_{ij} + 2\beta_{ij} - 2\beta_{i+1j} = 0 \quad (15)$$

Our last requirement is specific to the application of function fitting to robot motion planning, and it requires acceleration to be 0 at the initial and final state visited by the plan ρ . This requirement constraints are

$$2\beta_{0j} = 0 \quad (16)$$

$$6\alpha_{N-1j} + 2\beta_{N-1j} = 0 \quad (17)$$

It is easy to see that constraints (12)–(17) form a system of linear equations with $4d(N - 1)$ variables and constraints. When the constraints are linearly independent and consistent, there is a unique solution $\rho = a_0, \dots, a_i, \dots, a_{N-1}$.

6 Constraint Checking and Search Direction

We now define the checking procedures to produce cuts \mathcal{C}_k and \mathcal{V}_k , and how these are used to define the search directions used to select geometric graphs.

6.1 Exact Constraint Checking for Smooth Plans

The POLYTRACE algorithm [14, Algorithm 1] provides the means to test whether $\mathcal{B}_{\delta_i}(\rho) \cap O_i = \emptyset$, for a given polynomial $\rho : [0, 1] \rightarrow \mathbb{R}^d$ and region $O_i \subseteq \mathbb{R}^d$ described by (2). The test assumes that clearances δ_i are rational, and that all polynomials involved have rational coefficients: that is, $\rho \in \mathbb{Q}[t]^d$, each $g_j^i \in \mathbb{Q}[x_1, \dots, x_d]$, and $\delta_i \in \mathbb{Q}$.

Let us start by ignoring clearance constraints. The polynomial ρ intersects O_i , i.e. $\text{img}(\rho) \cap O_i \neq \emptyset$, iff exists k ,

$$\zeta(k) = \{1, \dots, m_i\} \quad (18)$$

where $\zeta := \text{POLYTRACE}(\rho, (g_1^i, \dots, g_{m_i}^i))$ is a *trace* [14, Definition 19], thus recording every region visited by ρ . To visit O_i , the polynomial ρ must simultaneously visit $\{x \in \mathbb{R}^d \mid g_j^i(x) \leq 0\}$ for every $1 \leq j \leq m_i$, as indicated by (18). We now reintroduce clearance requirements. We observe that

$$\mathcal{B}_{\delta_i}(\rho) \cap O_i = \emptyset \iff \text{img}(\rho) \cap (O_i \oplus \mathcal{B}_{\delta_i}(0)) = \emptyset \quad (19)$$

That is, the clearance constraint is satisfied iff ρ does not intersect $O_i \oplus \mathcal{B}_{\delta_i}(0)$, a δ_i -*expansion* of O_i . If we can find polynomials $h_j^i \in \mathbb{Q}[x_1, \dots, x_d]$ such that

$$O_i \oplus \mathcal{B}_{\delta_i}(0) \subseteq \bigcap_{i=1}^{m_i} \{x \in \mathbb{R}^d \mid h_j^i(x) \leq 0\}, \quad (20)$$

then the problem of determining whether $\mathcal{B}_{\delta_i}(\rho) \cap O_i$ is solved by examining $\zeta := \text{POLYTRACE}(\varphi, (h_1^i, \dots, h_{m_i}^i))$. If (18) fails to hold, then $\mathcal{B}_{\delta_i}(\rho) \cap O_i = \emptyset$, and sufficient clearance is guaranteed. In general, finding such h_j^i can be challenging. But if the g_j^i are affine, then (20) holds when we set

$$h_j^i(x) := g_j^i(x) - \delta_i c \quad (21)$$

for any $c \geq \|\nabla g_j^i(x)\|$. Recall that $\|\nabla g_j^i(x)\|$ is constant because g_j^i is affine. If we define $c := \|\nabla g_j^i(x)\|$, then (20) holds with equality, but then c is typically irrational, and leaves h_j^i having irrational coefficients. Choosing $c \in \mathbb{Q}$ to be a rational upper bound on $\|\nabla g_j^i(x)\|$ instead, guarantees $h_j^i \in \mathbb{Q}[x_1, \dots, x_d]$, as required. This introduces some conservativeness into the test.

We generate cuts \mathcal{V}_k (8) when we find an action a_j in ρ that satisfies condition (18), and \mathcal{V}_k is defined as

$$\mathcal{V}_k := \{e_l \in \pi_k : j_- \leq l \leq j_+\} \quad (22)$$

where $j_- = \max\{1, j-1\}$, $j_+ = \min\{j+1, N\}$ and $N = |\pi_k|$. If no such action a_j exists, then the statement $\text{img}(\rho) \subset F$ is proven to be true.

► **Remark 6.** Requiring every g_j^i to be affine restricts the regions O_i to either be polytopes, or the result of over-approximating each O_i with a polytope.

6.2 Managing Arithmetic Complexity

Applying POLYTRACE in the manner described in the previous section requires careful consideration of the arithmetic complexity of the calculations required. We identify and address two main challenges. First, all coefficients in constraints O_i and plans ρ must be rationals. Secondly, the time and space complexity of POLYTRACE [14, Algorithm 1] is dominated by that of finding the isolating intervals [15] for the roots of N products of polynomials that result from the composition of the right-hand side of constraints and each action $a_j \in \rho$. The result of this arithmetic operation, yet another polynomial, sometimes have very high degree and very large coefficients that cannot be represented with fixed-size data types native to computer programming languages. The parameters governing the growth of degree and maximal coefficient size of this product depend on the degree of the basis (section 5) used to define ρ and m_i . For instance, when using polytopes to represent constraints O_i and using the basis (10) with $l = 4$ on the instances discussed in section 7, we obtain fairly frequently polynomials of degree up to 16 with coefficients consisting of dozens of digits.

The first problem is overcome by computing rational approximations of coefficients of constraints O_i and actions a_j in plans ρ_k . Each floating-point number ξ representing a coefficient is mapped into a *dyadic rational* [30] ξ' , where the denominator is $d \in \mathbb{N}$, $1 \leq d \leq 2^\beta$ ³. ξ' is selected so as to minimize $|\xi - \xi'|$ and the bitsize of d . Using small powers of two as denominators greatly reduces the bit complexity of the arbitrary precision arithmetic operations required to implement POLYTRACE⁴.

► **Remark 7.** Alternatively, and when performance is not a concern, a Computer Algebra System such as MATHEMATICA [31] or SYMPY [32] can be readily used to implement POLYTRACE.

The second problem required to analyze how the truth of each *relational atom* $\alpha_{il} \equiv (g_i^l \circ \rho_j(t)) \leq 0$ changes through the actions ρ_j in the incumbent smooth plan. For that we borrow the notion of *inertial atoms* [33], and observe that existence of *any* roots for a polynomial ρ_j in a interval I can be determined by means of *Descartes' sign rule* [15]. Thus, for every action ρ_j in the plan, we can

³ In this paper, $\beta = 14$, which results in an approximation down to the fourth decimal place of floating-point numbers ξ .

⁴ We use the `boost::cpp_int` library for this.

evaluate the truth of α_{il} at $a_j(0)$ and $a_j(1)$, and if Descartes' rule certifies that no roots exist in the interval $(0, 1)$, then we know α_{il} is *inertial*, e.g. its truth value remains constant within the $[0, 1]$ interval, and does not need to be considered in any calls to POLYTRACE to obtain traces ζ_j . This simple and efficient test very often greatly reduces the complexity of product polynomials when O_i is a polytope.

6.3 Velocity and Kinematic Constraints

Following [19, Chapter 13], we now assume that C specifies the possible configurations of one or more rigid bodies. As discussed in section 2.1, plan domain Π is given by m' *implicit differential constraints* 4 on plans $\rho : [0, 1] \rightarrow C$. As long as each $g_i \circ \rho$ in 4 are polynomials in $\mathbb{R}[t]^d$, we can use POLYTRACE to generate a trace ζ as we did to check geometric constraints in section 6.1. We then can establish that $\rho \in \Pi$ if for all $k = 1, \dots, |\zeta|$ it holds that $|\zeta(k)| = m$. In words, at no point $t \in [0, 1]$ we found $\rho(t)$ to be somewhere else than inside the region in tangent space enclosed by the boundaries of constraints g_i in (4). A cut constraint \mathcal{C}_k (8) follow from actions a_j in ρ that do not satisfy (4)

$$\mathcal{C}_k := \{e_l \in \pi_k : j_- \leq l \leq j_+\} \quad (23)$$

where j_-, j_+ and N are as in (22).

When $g \circ \rho$ is not a polynomial, we can still define useful cuts, but only at specific points along plans ρ . We illustrate this with the following constraints. Let us suppose $C = \mathbb{R}^2$, and ρ is a piece-wise C^2 -continuous function obtained as per Section 5. We set the following constraint for each action a_j in ρ , and intervals $I = (l, r) \in \{(0, 1/2), (1/2, 1)\}$

$$-\phi_{max} \leq \arccos\left(\frac{\dot{a}_j(r) \cdot \dot{a}_j(l)}{\|\dot{a}_j(r)\| \|\dot{a}_j(l)\|}\right) \leq \phi_{max} \quad (24)$$

where ϕ_{max} is the largest allowed change in the direction of the tangent of plan ρ along actions a_j . Constraint (24) is useful to model limits on steering angles for a wide family of robotic systems [34]. If some action(s) a_j do not satisfy constraints (24) then cuts \mathcal{C}_k as above (23) are generated.

6.4 Directing the Search for Geometric Graphs

As advanced in section 3 we use a dynamic sampling sequence \mathcal{X} (section 2.2) where random variables X_k for iteration k are use the information conveyed by cuts \mathcal{V}_j and \mathcal{C}_j , for $j < k$, directing the selection of graph G_k .

For each cut \mathcal{V}_j and \mathcal{C}_j generated up to iteration k , *search directions* (distributions) \mathcal{N}_j are defined following Bohlin and Kavraki [5], but with *seed states* q_j defined to be the barycenter of vertices $q_i, q_{i'} \in V_j$ at endpoints of edges $x_{ii'}$ in cuts (8). This heuristic exploits the observation that cubic splines lack *localism* [29]. By choosing new vertices from \mathcal{N}_j we will be generating plans ρ_k that are close perturbations of previously rejected plans ρ_j .

7 Evaluation

7.1 Benchmarks and Execution Environment

We illustrate and evaluate the performance of our Lazy PRM algorithm on the BARN dataset, a publicly available benchmark for robotic motion planning tasks [18] that also have a clear pathway for implementation on easily accessible high-fidelity simulation and robotic hardware. We use the 300 instances available here [35], that represent freespace F using Robot Operating System (ROS) [36]

occupancy grids. We map these into sets of (possibly overlapping) polytopes automatically via a simple greedy approximation of the problem given in [37, Section 2]. This procedure is written in Python, and we observed it takes well below one second to process each instance in the set [35]. The size of the resulting geometric constraint sets O ranges from 30 to 70 sets O_i , their boundaries described by 4 to 6 affine constraints. We impose constraint (24), with maximum angle ϕ_{max} is $\pi/2$ (90°). Initial and goal states are the same in every instance and chosen so that non-trivial tasks (e.g. ρ has $N > 1$ actions) are generated with high probability⁵.

We ran our planners (written in C++) in Ubuntu 20.04, over an 8-core 11th Generation Intel Processor with a clock speed of 3.6GHz. For each instance (e.g. definition of F , q_0 and F_*), we do 5 runs, using numbers 1, 42, 567, 1337 and 8193 to seed random number generators. Runs are terminated after 500 seconds or earlier if a suboptimal solution of Problem (3) is found. Reported timing information follows from measurement by the `steady_clock` available through the `chrono` C++ standard library module. Runs working set is limited to 4 GBytes of RAM.

7.2 Planners

We have tested two implementations of the Lazy PRM scheme described in Figure 3, that differ in the choice of algorithm to solve the CMCP problem described in section 4. The first algorithm is Google’s CP-SAT Branch-and-Bound solver [38] that combines state-of-the-art techniques for Constraint Programming (CP) and Mixed-Integer Programming (MIP), using Lazy Clause Generation (LCG) [39]. The second algorithm is a bespoke two-tiered Dynamic Programming (DP) algorithm that uses Euclidean distance as a lower bound [40]. This algorithm uses A^* [41] to solve instances of Problem (7), and switches to Best-First Search [27, Chapter 5] when cuts (8) have been added. The latter algorithm lazily checks that cuts are satisfied before a path (node) selected from the search frontier is expanded.

► **Remark 8.** The reason for switching from A^* follows from the observation that pruning paths $p \in Paths(G)$ from vertex q_0 when these do not satisfy some active cut (8) violates a key assumption in A^* . To wit, whenever a partial path p between q_0 and a vertex q is added to the open list, we will not need to consider any other path from q_0 that visits q , and thus any such alternatives can be pruned away. This is violated when \mathcal{V}_k contains multiple edges, as the vertex q may be reached through different edges, not featured on any active cut constraint. In order to use A^* , one would need to consider an extended graph $G' = (V', E')$ defined as follows. The vertex set V' would be given by $V' := V \times \mathbb{Z}_0^{k+}$, the Cartesian product between the vertex set of the geometric graph and the set of integer vectors with non-negative elements, and initial vertex $v_0 \in V'$ is the pair $(q_0, \mathbf{0})$. Given cuts \mathcal{V}_k and \mathcal{C}_k , the edge set $E' \subset V' \times V'$ would consist of edges $e = (v, v')$ where $v = (q, z)$ and $v' = (q', z')$ that satisfy the following conditions:

1. vertices q and q' were connected already in G , e.g. $(q, q') \in E$,
2. $z'_j = z_j + 1$ if $(q, q') \in \mathcal{V}_j$, or $(q, q') \in \mathcal{C}_j$, for $1 \leq j \leq k$, otherwise $z_j = z'_j$,
3. $z'_j \leq \max\{|\mathcal{V}_j|, |\mathcal{C}_j|\}$ for $1 \leq j \leq k$.

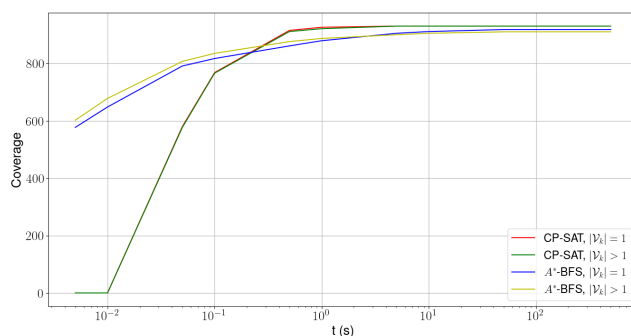
Constructing these augmented graphs G' imposes significant computational burdens, even when using compact representations for E such as STRIPS operators [42, 43] as the geometric graphs G and number of cuts k to consider grows with each iteration. Also, sophisticated data structures become necessary to implement efficiently the open and closed lists.

For each planning algorithm we tested two different definitions of \mathcal{X} . In addition to any generated neighborhoods \mathcal{N}_j , $j = 0, \dots, k - 1$, we consider two undirected sampling strategies. One is to

⁵ We refer the reader to the videos available here: <https://bit.ly/3rbGPGGr>

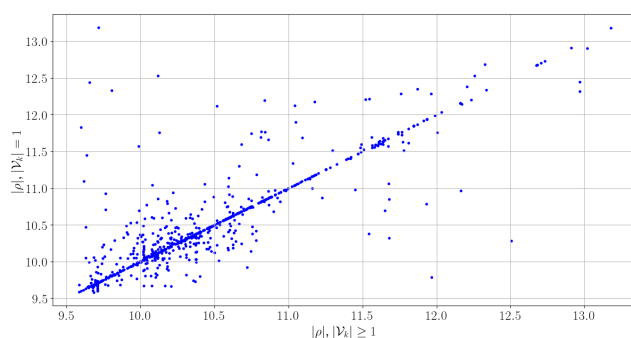
sample a uniform distribution over F , the other is to enumerate the Halton sequence. We compare Bohlin and Kavragi [5] definition of seed states, with the one proposed in section 6.4, as the latter considers multiple edges in generated cuts. We start by generating a geometric graph G_0 with 20 vertices, and whenever no solutions are found for Problem (7) over graph G_k , we add 10 new vertices to obtain G_{k+1} , 5 from a randomly chosen neighborhoods \mathcal{N}_j , the other from the undirected samplers.

7.3 Overview of Results



■ **Figure 4** Coverage (number of runs finding one solution) over time for CP-SAT and A^* -BFS planners, using deterministic undirected sampling, and either single or multiple-edge cuts. See text for discussion.

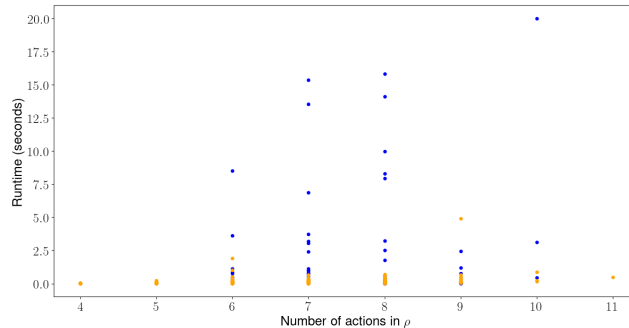
Figure 4 show the *coverage over time* curves for the planners with highest coverage (number of solved instances within time limits) and best quality plans. Planners based on CP-SAT solved all 1,500 instances, and we found DP-based ones to run out of memory in about 1% of them. This event is significantly more frequent when using uniform undirected sampling. CP-SAT has a significant overhead when starting up: this follows from us relying on the (default) solver interface designed for distributed applications, that marshalls the variables and constraints of Problem (7) to be transmitted over a network. Much lower initial latency is possible by using directly CP-SAT low-level data structures. Trajectory fitting (section 5) and checking of kinematic constraints (24) have negligible impact on runtimes. Geometric constraint verification takes up 80% of the runtime on average, the other 20% being spent finding minimum-cost paths over G_k . We observed a significant difference



■ **Figure 5** Approximate arc-lengths of plans ρ for multi (x-axis) and single-edge (y-axis) cuts \mathcal{V}_k , when using deterministic undirected sampling.

when using single and multiple-edge cuts \mathcal{V}_k when it comes to plan costs, obtained from the numeric integration of the arc-length for smooth plans ρ . Figure 5 shows that for most of runs, there is no cost difference, but when using larger cuts \mathcal{V}_k lower cost plans are often obtained. More often we observe

that using larger cuts results in smaller differences in costs w.r.t. the minimum cost observed. In Figure 5 we show the results when using the Halton sequence to define \mathcal{X} , and the observed trend is noticeably amplified when using uniform random sampling. Finally, we compare in Figure 6 A^* -BFS



■ **Figure 6** Number of actions in plans ρ and run-time of planners. Blue is for A^* -BFS planner, orange for CP-SAT.

and CP-SAT runtimes as the number of actions in plans ρ increases. DP planners are significantly faster in runs where a valid plan ρ was found after a few iterations, graphs are small and plans do not have many actions (75% of instances admit valid plans with ≤ 6 actions, and the shortest ρ observed has 4 pieces). CP-SAT runtime does not degrade as plans get longer. As the lower bound directing A^* -BFS becomes less informed due to paths being removed from G_k , the more likely is BFS to devolve into Dijkstra’s algorithm with the added overheads of more complex data-structures and lower bound evaluations.

These results⁶ provide compelling evidence of the practical feasibility of our Lazy PRM algorithm (Figure 3). The probability of producing a valid smooth plan ρ under 1 second is very high, on the benchmark considered here.

8 Related Work

Existing work on kinodynamic motion planning typically relies on discretizing trajectories to check validity of plans [5, 44, 45], or require a triangulation of F into convex pieces [44, 46, 47]. A recent exception to this is the work of Zhang et al. [48], who propose the notion of Kinodynamic Networks, geometric graphs (section 2.2) where Λ are Cubic Bézier curves. A curve is admitted into the definition of Λ whenever its endpoints are vertices in the network and the convex hull of its control points does not overlap any O_i . At the time of writing this we are not aware of published analysis showing this approach to be AO or PC. The Lazy PRM algorithm in Figure 3 is both AO and PC, and this follows directly from the theory developed for probabilistic roadmaps [10, 11, 22].

Conceptually close but methodologically distant to this paper is the recent work of Ortiz-Haro et al. [49] based on the Logic Geometric Programming (LGP) framework of M. Toussaint [50]. Ortiz-Haro et al. propose to compile via polynomial-time reduction instances of Problem (7) into a discrete deterministic planning problem [19, Section 2.4]. Their approach relies on very scalable methods for the latter class of optimal discrete control problems. Ortiz-Haro et al. do not provide near-optimality guarantees, and the overheads of representing the constraints of Problem (7) as STRIPS operators are substantial

⁶ The evaluation data along with JUPYTER notebooks calculating these and other statistics can be found on the following link: <https://bit.ly/3B007H2>.

Lastly, the recent results showing Branch-and-Cut and other advanced techniques for Integer programming to be a highly performing approach to Multi-Agent Path Planning problems [51] were a direct inspiration to us. As it has long been recognized in the literature [23, 52], the gap between so-called “grid-based” and sampling-based motion planning “just” lies in the provenance and properties of the underlying geometric graphs both methodologies use.

9 Future Work

We look forward to study the relation between algorithms for Problem (6) like PRM and the Dantzig-Wolfe decomposition for linear programming [16, 53], developing theory to analyse possible connections between state-of-the-art motion planning algorithms and classic results in optimization. We are also interested in further pursuing the research into the synthesis of motion plans that satisfy LTL specifications initiated in the classic work by Bhatia et al. [44], and to explore the potential of motion planning algorithms using POLYTRACE into model checking for hybrid control systems [54]. Our approach supports a very general class of geometric differential constraints of arbitrary order, those that are expressed as systems of polynomial equations. We look forward to investigate the behaviour of the branch-and-cut planning algorithm proposed in this paper over more varied sets of constraints and uncertainty [55].

Acknowledgment

The authors would like to thank the Australian Government through Trusted Autonomous Systems, a Defence Cooperative Research Centre under the Next Generation Technologies Fund.

References

- 1 R. Hettich and K. O. Kortanek, “Semi-infinite programming: Theory, methods and applications,” *SIAM Review*, vol. 35, no. 3, pp. 380–429, 1993.
- 2 B. Donald, P. Xavier, J. Canny, and J. Reif, “Kinodynamic motion planning,” *Journal of the Association for Computing Machinery*, vol. 40, no. 5, pp. 1048–1066, 1993.
- 3 A. D. Ames, S. Coogan, M. Egerstedt, G. Notomista, K. Sreenath, and P. Tabuada, “Control barrier functions: Theory and applications,” in *18th European Control Conference (ECC)*. IEEE, 2019.
- 4 M. J. Van Nieuwstadt and R. M. Murray, “Real-time trajectory generation for differentially flat systems,” *International Journal of Robust and Nonlinear Control*, vol. 8, no. 11, pp. 995–1020, 1998.
- 5 R. Bohlin and L. E. Kavraki, “Path planning using lazy PRM,” *Proceedings 2000 ICRA. Millennium Conference. IEEE International Conference on Robotics and Automation*, vol. 1, pp. 521–528, 2000.
- 6 M. Penrose, *Random Geometric Graphs*. Oxford University Press, 2003.
- 7 B. Korte and J. Vygen, *Combinatorial Optimization: Theory and Algorithms*, 6th ed. Springer, 2018.
- 8 M. Bruynooghe, “Solving combinatorial search problems by intelligent backtracking,” *Information Processing Letters*, vol. 12, no. 1, 1981.
- 9 J. N. Hooker, *Integrated Methods for Optimization*. Springer, 2010.
- 10 S. Karaman and E. Frazzoli, “Sampling-based algorithms for optimal motion planning,” *The International Journal of Robotics Research*, vol. 30, pp. 846–894, 2011.
- 11 K. Solovey, L. Janson, E. Schmerling, E. Frazzoli, and M. Pavone, “Revisiting the asymptotic optimality of RRT,” in *2020 IEEE International Conference on Robotics and Automation (ICRA)*, 2020, pp. 2189–2195.
- 12 A. Tarski, *A Decision Method for Elementary Algebra and Geometry*, 2nd ed. University of California Press, 1951.
- 13 D. S. Dummit and R. M. Foote, *Abstract Algebra*. Wiley, 2004.
- 14 D. Selvaratnam, M. Cantoni, J. M. Davoren, and I. Shames, “Sampling polynomial trajectories for LTL verification,” *Theoretical Computer Science*, vol. 897, pp. 135–163, Jan 2022.

- 15 K. Mehlhorn and M. Sagraloff, "A deterministic algorithm for isolating real roots of a real polynomial," *Journal of Symbolic Computation*, vol. 46, no. 1, pp. 70–90, 2011.
- 16 L. A. Wolsey and G. L. Nemhauser, *Integer and Combinatorial Optimization*. Wiley Interscience, 1999.
- 17 J. E. Mitchell, "Branch-and-Cut Algorithms for Combinatorial Optimization Problems," in *Handbook of Applied Optimization*. Oxford University Press, 2000.
- 18 D. Perille, A. Truong, X. Xiao, and P. Stone, "Benchmarking metric ground navigation," in *2020 IEEE International Symposium on Safety, Security and Rescue Robotics (SSRR)*. IEEE, 2020.
- 19 S. M. LaValle, *Planning Algorithms*. Cambridge University Press, 2006.
- 20 L. Kavraki, P. Svestka, J.-C. Latombe, and M. Overmars, "Probabilistic roadmaps for path planning in high-dimensional configuration spaces," *IEEE Transactions on Robotics and Automation*, vol. 12, no. 4, 1996.
- 21 L. E. Kavraki, M. Kolountzakis, and J.-C. Latombe, "Analysis of probabilistic roadmaps for path planning," *IEEE Transactions on Robotics and Automation*, vol. 14, no. 1, pp. 166–171, 1998.
- 22 K. Solovey and M. Kleinbort, "The critical radius in sampling-based motion planning," *The International Journal of Robotics Research*, vol. 29, no. 2–3, pp. 266–285, 2020.
- 23 L. Janson, B. Ichter, and M. Pavone, "Deterministic sampling-based motion planning: Optimality, complexity, and performance," *International Journal of Robotics Research*, vol. 37, no. 1, pp. 46–61, 2018.
- 24 S. Boyd and L. Vandenberghe, *Convex Optimization*. Cambridge University Press, 2004.
- 25 M. Moskewicz, C. Madigan, Y. Zhao, L. Zhang, and S. Malik, "Chaff: engineering an efficient SAT solver," *Proceedings of the 38th Design Automation Conference*, pp. 530–535, 2001.
- 26 R. Kipp-Martin, *Large Scale Linear and Integer Optimization*. Kluwer Academic Press, 1999.
- 27 D. P. Bertsekas, *Dynamic Programming and Optimal Control*, 4th ed. Athena Scientific, 2017, vol. 1.
- 28 M. Grötschel and M. W. Padberg, "On the symmetric travelling salesman problem I: inequalities," *Mathematical Programming*, no. 16, pp. 265–280, 1979.
- 29 C. Sprunk, "Planning motion trajectories for mobile robots using splines," <http://www2.informatik.uni-freiburg.de/~lau/students/Sprunk2008.pdf>, Albert-Ludwigs-Universität Freiburg, Tech. Rep., 2008.
- 30 D. E. Knuth, *The Art of Computer Programming, Volume 2 (3rd Ed.): Seminumerical Algorithms*. Addison-Wesley Longman Publishing Co., 1997.
- 31 W. R. Inc., "Mathematica, Version 13.1," champaign, IL, 2022. [Online]. Available: <https://www.wolfram.com/mathematica>
- 32 A. Meurer, C. P. Smith, M. Paprocki, O. Čertík, S. B. Kirpichev, M. Rocklin, A. Kumar, S. Ivanov, J. K. Moore, S. Singh, T. Rathnayake, S. Vig, B. E. Granger, R. P. Muller, F. Bonazzi, H. Gupta, S. Vats, F. Johansson, F. Pedregosa, M. J. Curry, A. R. Terrel, v. Roučka, A. Saboo, I. Fernando, S. Kulal, R. Cimrman, and A. Scopatz, "SymPy: symbolic computing in python," *PeerJ Computer Science*, vol. 3, p. e103, Jan. 2017. [Online]. Available: <https://doi.org/10.7717/peerj-cs.103>
- 33 E. Giunchiglia, J. Lee, V. Lifschitz, N. McCain, and H. Turner, "Nonmonotonic causal theories," *Artificial Intelligence*, vol. 153, no. 1-2, pp. 49–104, 2004.
- 34 J.-P. Laumond, S. Sekhavat, and F. Lamiroux, "Guidelines in nonholonomic motion planning for mobile robots," in *Robot Motion Planning and Control*. Springer, 1998, pp. 1–53.
- 35 X. Xuesu, "Benchmarks for autonomous robot navigation (barn)," <https://www.cs.utexas.edu/~xiao/BARN/BARN.html>, 2022, accessed 26/08/22.
- 36 Stanford Artificial Intelligence Laboratory et al., "Robotic operating system." [Online]. Available: <https://www.ros.org>
- 37 A. Bemporad, C. Filippi, and F. D. Torrisi, "Inner and outer approximations of polytopes using boxes," *Computational Geometry*, vol. 27, no. 2, pp. 151–178, 2004.
- 38 L. Perron and V. Furnon, "Or-tools," Google. [Online]. Available: <https://developers.google.com/optimization/>
- 39 O. Ohrimenko, P. J. Stuckey, and M. Codish, "Propagation via lazy clause generation," *Constraints*, vol. 14, no. 3, pp. 357–391, 2009.
- 40 J. Pearl, *Heuristics: Intelligent Search Strategies for Computer Problem Solving*. Addison-Wellesley, 1984.

- 41 P. E. Hart, N. J. Nilsson, and B. Raphael, "A formal basis for the heuristic determination of minimum cost paths," *IEEE transactions on Systems Science and Cybernetics*, vol. 4, no. 2, pp. 100–107, 1968.
- 42 R. E. Fikes and N. J. Nilsson, "STRIPS: A new approach to the application of theorem proving to problem solving," *Artificial Intelligence*, vol. 2, no. 3-4, pp. 189–208, 1971.
- 43 G. Frances and H. Geffner, "Modeling and computation in planning: Better heuristics from more expressive languages," in *ICAPS*, 2015.
- 44 A. Bhatia, L. E. Kavraki, and M. Y. Vardi, "Sampling-based Motion Planning with Temporal Goals," *2010 IEEE International Conference on Robotics and Automation*, pp. 2689–2696, 2010.
- 45 J. Schulman, Y. Duan, J. Ho, A. Lee, I. Awwal, H. Bradlow, J. Pan, S. Patil, K. Goldberg, and P. Abbeel, "Motion planning with sequential convex optimization and convex collision checking," *The International Journal of Robotics Research*, vol. 33, no. 9, pp. 1251–1270, 2014.
- 46 E. Plaku and G. D. Hager, "Sampling-based motion and symbolic action planning with geometric and differential constraints," in *Proc. of the IEEE Conference on Robotics and Automation (ICRA)*, 2010.
- 47 Y. Shoukry, P. Nuzzo, A. Balkan, I. Saha, A. L. Sangiovanni-Vicentelli, S. E. Seshia, G. J. Pappas, and P. Tabuada, "Linear temporal logic motion planning for teams of underactuated robots using satisfiability modulo convex programming," in *IEEE International Conference on Decision and Control*, 2017.
- 48 H. Zhang, N. Tiruvilumala, S. Koenig, and T. K. S. Kumar¹, "Temporal Reasoning with Kinodynamic Networks," in *Proceedings of the Thirty-First International Conference on Automated Planning and Scheduling*, 2021.
- 49 J. Ortiz-Haro, E. Karpas, M. Katz, and M. Toussaint, "A Conflict-driven Interface between Symbolic Planning and Nonlinear Constraint Solving," *IEEE Robotics and Automation Letters*, vol. PP, no. 99, pp. 1–8, 2022.
- 50 M. Toussaint, "Logic-geometric programming: An optimization-based approach to combined task and motion planning," in *IJCAI*, 2015.
- 51 E. Lam, P. L. Bodic, D. Harabor, and P. J. Stuckey, "Branch-and-cut-and-price for multi-agent pathfinding," in *Proceedings of the Twenty-Eighth International Joint Conference on Artificial Intelligence (IJCAI-19)*, 2019.
- 52 S. M. LaValle, M. S. Branicky, and S. R. Lindemann, "On the relationship between classical grid search and probabilistic roadmaps," *International Journal of Robotics Research*, vol. 23, no. 7–8, pp. 673–692, 2004.
- 53 VVAA, *Column Generation*, G. Desaulniers, J. Desrosiers, and M. M. Solomon, Eds. Springer, 2005.
- 54 L. Doyen, G. Frehse, G. J. Pappas, and A. Platzer, "Verification of hybrid systems," in *Handbook of Model Checking*, E. E. Clarke, T. A. Henzinger, H. Veith, and R. Bloem, Eds. Springer, 2018.
- 55 K. E. Bekris and L. E. Kavraki, "Greedy but safe replanning under kinodynamic constraints," in *Proceedings of IEEE Conference on Robotics and Automation (ICRA)*, 2007.